Localized Metallic Conductivity and Self-Healing during Thermal Reduction of $SrTiO_3$

K. Szot,[1] W. Speier,[2] R. Carius,[3] U. Zastrow,[3] and W. Beyer[3]

[1]*Institut für Festkörperforschung, Forschungszentrum Jülich, 52425 Jülich, Germany*
[2]*Institut für Chemie und Dynamik der Geosphäre, Forschungszentrum Jülich, 52425 Jülich, Germany*
[3]*Institut für Photovoltaik, Forschungszentrum Jülich, 52425 Jülich, Germany*

(Received 25 June 2001; published 1 February 2002)

The occurrence of metallic conductivity in $SrTiO_3$ single crystals is reported for reduction under low partial pressure of oxygen at 800 °C. This transition is shown to result from the formation of a high concentration of vacancy defects along a network of extended defects within the skin region. A self-healing phenomenon is observed for progressive reduction which causes the concentration of initially introduced defects to decrease in the course of heat treatment and leads to a breakdown of the metallic conductivity as well as a substantial loss of optical subgap absorption.

DOI: 10.1103/PhysRevLett.88.075508 PACS numbers: 61.72.–y, 66.30.–h, 71.30.+h, 78.68.+m

Ternary oxides with perovskite structure show a wide span of electrical properties with doping, ranging from insulating, semiconducting to metallic and even superconducting behavior. This has found a resurgence of interest in conjunction with electron correlation effects in transition metal oxides [1] and due to the close structural relation of the perovskites with high-T_c superconductors [2]. Thermal reduction of the oxides, sometimes also termed self-doping, is a particularly effective means to dope electrons as charge carriers into the system by a thermally induced modification of the composition and corresponding generation of oxygen vacancy defects. In this respect, $SrTiO_3$ is regarded as a prototype perovskite [3]: it shows an insulator-to-metal transition [4] and was the first discovered to exhibit superconductivity [5]. However, the transition from insulating to metallic behavior in this material occurs at an extremely small critical density of electron doping (around 10^{18} cm^{-3}), which is several orders of magnitude below the typical values found for substituted transition metal oxides [3]. This unusual behavior has been related to the high dielectric constant and discussed as an example case of the applicability of the Mott criterion [3]. Similarly, superconductivity occurs at a relatively low value of charge carrier concentration (around 10^{19} cm^{-3}) [4,6] or low density of states at the Fermi energy [7].

The analysis of the electrical properties as a result of thermal reduction under equilibrium conditions regards $SrTiO_3$ as a homogeneous material. The related density of introduced charge carriers is then taken to be characteristic for the bulk and considered as a volume property. However, very recent studies bring into focus the special role of the dislocations of the single crystalline material. Dislocations are responsible for the ductile behavior of $SrTiO_3$ single crystals at room as well as elevated temperature [8]. Work by Wang, Zhu, and Shapiro [9] has even revealed that the "skin" region of $SrTiO_3$ shows an increased density of dislocations with respect to the bulk of the crystal. As the equilibration kinetics under reducing conditions is controlled by the diffusivity of oxygen within the crystal, the dislocations constitute a medium of lower dimensionality which provide easy diffusion paths [10,11]. The dislocations in the skin region are also accompanied by a highly distorted lattice [9] which may give rise to additional cation segregation [12]. Even more, nonperovskite phases have been observed to develop on and in close proximity to the surface at elevated temperatures [13]. This raises the question of the influence of the structural and chemical character of the skin region on the thermal reduction process and related macroscopic properties.

In this Letter we give evidence that the structural character of $SrTiO_3$ single crystals allows for a transition to metallic conductivity under reducing conditions which have been hitherto considered to introduce oxygen vacancy defects in the dilute limit and to result in only semiconducting behavior. However, this metallic state is shown to break down using prolonged reduction as a result of a self-healing phenomenon which decreases dramatically the density of initially introduced vacancy defects and related charge carriers.

Measurements were conducted on standard (undoped) Verneuil-grown single crystals of $SrTiO_3$ with a nominal (100) orientation available from CrysTec (Berlin) and MaTeck (Jülich). Thermal reduction was performed with a standard ultrahigh-vacuum system at a partial pressure of oxygen of 10^{-8} Torr with temperatures in the range of 700 to 1000 °C. The partial pressure of oxygen was maintained by a controlled inflow of high-purity oxygen or Ar/H_2-mixture and continuously monitored by a quadrupole mass spectrometer. All measurements have been undertaken on samples (as-received polished, cut, or cleaved) which have not been subjected to any heat treatment prior to measurement ("virgin crystals").

The density of dislocations at the surface of the crystals under investigation was determined by atomic force microscopy (AFM) after light chemical etching in HCl. Figures 1a and 1b show different locations on the same sample with a similar density of etch pits of the order of $4 \pm 1 \times 10^9$ cm^{-2}, close to values found by others for surfaces of the same orientation [14]. A distinct alignment or aggregation of dislocations can be observed, typically

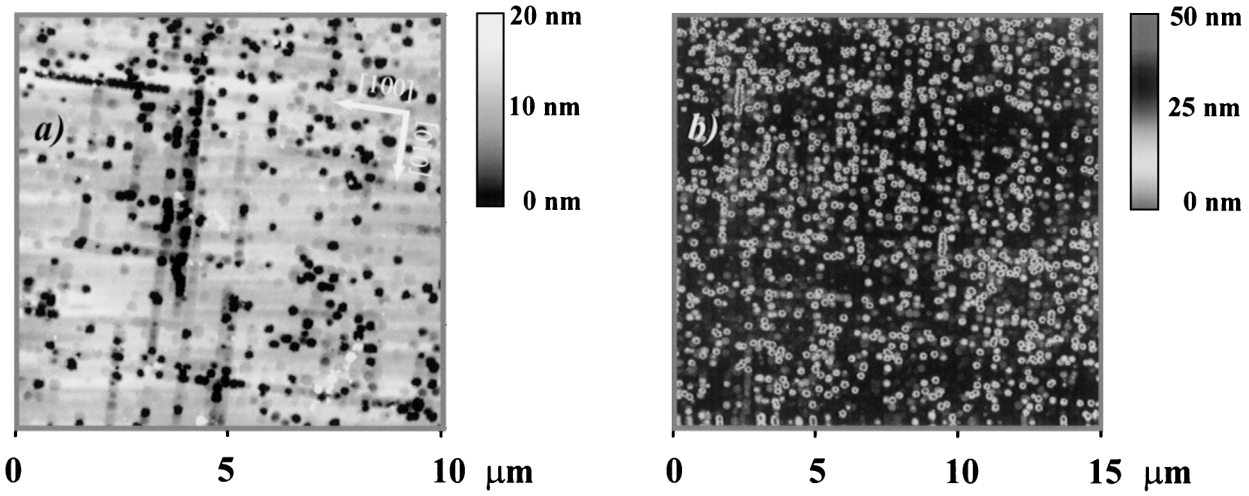

FIG. 1. AFM of two different locations of etched (100) surfaces of $SrTiO_3$ (a),(b) with an estimated density of dislocations of the order of 4×10^9 cm^{-2}.

along the [100] direction. This alignment of dislocations along a crystallographic direction is also apparent in x-ray topographical studies [15] analogous to $KNbO_3$ [16]. The density of dislocations for our polished surfaces is close to the values found by Wang, Zhu, and Shapiro [9] for the surface of (unpolished) cut samples (6×10^9 cm^{-2}). For the samples under investigation we therefore presume a three-dimensional network of dislocations within the skin region being characterized by the empirical density distribution determined by Wang, Zhu, and Shapiro for the first tens of μm [9].

The dislocations provide easy diffusion paths for oxygen, which becomes readily apparent from depth profile measurements by secondary ion mass spectrometry (SIMS) in conjunction with penetration experiments utilizing ^{18}O tracer. For this, samples were first reduced under high-vacuum conditions and then subjected *in situ* at the same temperature ($T = 800\,^{\circ}$C) to an ^{18}O-enriched atmosphere (97.26% at 50 mbar). The depth distribution of incorporated oxygen in the form of ^{18}O for different penetration times (Fig. 2) are characteristic for an enhanced diffusion along preferential paths which allows deep penetration analogous to $CaTiO_3$ [17] or $KNbO_3$ [16]. The intensity profiles c follow closely the relationship by Fisher-Suzuoka-Le Claire (see [10], and references therein), with $\partial \log c / \partial z^{6/5}$ proportional to $(tD_{\mathrm{disl}}^2/D_{\mathrm{latt}})^{-0.3}$ where z is the penetration depth, t the penetration time, and D_{latt} and D_{disl} the diffusion coefficients for the regular lattice and along dislocations, respectively. From the depth profiles we can extract the corresponding diffusion coefficients $D_{\mathrm{latt}} = 10^{-15}$ cm^2 s^{-1} and $D_{\mathrm{disl}} = 10^{-11}$ cm^2 s^{-1}. In fact, the latter is in good agreement with the values extrapolated from experiments by Paladino *et al.* [11] which analyze the tracer depletion in the gas phase. Even more, our depth profiles reveal diffusion along an array of dislocations since the slope of the profiles follows closely the time dependence with penetration time according to the above given relationship (see Fig. 2b [10,18]).

Effusion experiments at 800 °C (for details of the experimental procedure see [19]) allow one to estimate the amount of oxygen released from $SrTiO_3$ under vacuum conditions. Figure 3a shows that most of the oxygen is released from the samples within short times (already within 5 min) and that the amount of oxygen based on the total sample volume does not exceed 3×10^{14} cm^{-3} $\pm$ 20%. These results confirm that thermal reduction of $SrTiO_3$ is a highly efficient means with a drastic drop in electrical resistivity (Fig. 3b) by around 10 orders of magnitude with respect to the original sample within a short period. The corresponding electrical conductivity reveals metallic behavior on cooling (see Fig. 3c). The observed low resistivity is not limited to the outmost surface or its close proximity. In fact, one has to remove substantial portions of our samples, at least 5–10 μm, before decreasing

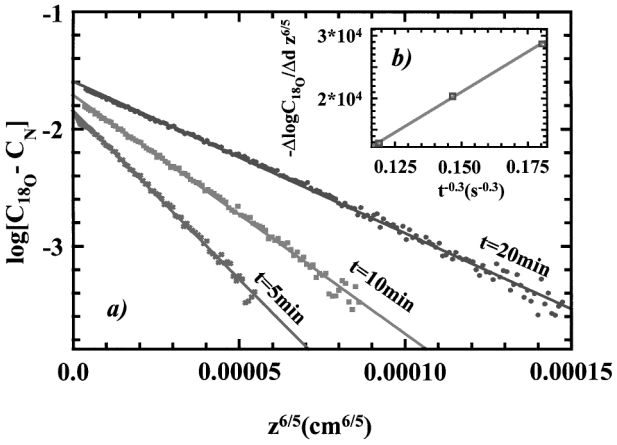

FIG. 2. The fraction of ^{18}O as detected by SIMS for reduced $SrTiO_3$ reoxidized in an ^{18}O-enriched atmosphere for different penetration times ($t = 5, 10, 20$ min). The natural ^{18}O isotope fraction c_N is subtracted. The axes are chosen such that the data exhibit straight lines for diffusion along dislocations. The slope of the profiles as a function of penetration time (see inset) reveal diffusion along dislocations grouped in sub-boundaries (network).

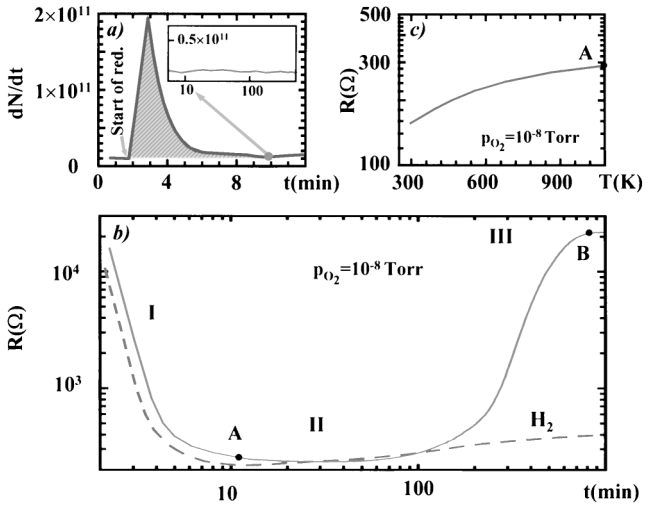

FIG. 3. Equilibration kinetics for thermally reduced $SrTiO_3$ under vacuum conditions ($p_{O_2} = 1 \times 10^{-8}$ Torr, $T = 800$ °C) monitored by the oxygen lost from the sample by effusion measurements (a) and independent measurements of the electrical resistivity (b). Cooling samples after heat treatment at point *A* reveals metallic behavior down to room temperatures (c). The sample reduced under H_2-enriched atmosphere (dashed line) at the same partial pressure of oxygen shows a similar trend, though markedly different in absolute values for extensive reduction.

dramatically the electrical conductivity (measured by a standard four-probe method, Valdes technique). Employing various materials for the electrical contact gives only marginal differences as long as the preparation of the electrodes does not involve modifications of the surface such as sputtering of heat treatment.

The kinds of conditions applied in the present work are generally considered in the standard defect chemical analysis of $SrTiO_3$ to correspond to the dilute limit of induced vacancy concentration and to allow for only *n*-type semiconducting behavior (see, e.g., [20–23]). So far, effects due to disorder have been discussed mainly for highly oxygen-deficient crystals [24,25]. On the other hand, Calvani *et al.* [4] have suggested considering the coexistence of metallic (disordered) and insulating portions of the crystal near the insulator-to-metal transition of $SrTiO_3$ as a consequence of fluctuations in the defect density. Our results show that the relevant densities of charge carriers are grossly underestimated by relating the electrical conductivity in a standard manner with respect to the volume. We can estimate the local concentration of introduced vacancy defects by combining the available information for the dislocation density, the diffusion coefficients, and the total amount of oxygen released. One obtains a lower bound for the local density of oxygen vacancies of 2×10^{20} cm^{-3} by assuming a homogeneous distribution of vacancy states within a cylindrical volume surrounding the dislocations for a situation where most of the oxygen has been released (e.g., point *A*). Such concentration of defects gives rise to carrier concentrations well above the supposedly critical threshold for the insulator-to-metal transition [4] or Mott criterion for this material [3]. *Ab initio* band structure calculations for this kind of defect densities are available and position the Fermi energy well into the conduction band of mainly Ti *d* character [26]. The same holds true for oxygen-deficient dislocations at grain boundaries [27]. The finite density of band states at the Fermi energy prevails also in those cases where clustering of vacancies [26] or correlation effects within an inhomogeneous Hubbard-like model [25] are taken into account. Therefore, the observed metallic conductivity is describable by a delocalization of charge carriers within the conduction band along an interconnected network of extended defects [28] which "short-circuits" the electrical properties of the insulating lattice.

However, the electrical resistivity (Fig. 3b) does not establish a stable plateau, as would be expected for reaching equilibrium conditions [22], but rather goes through a minimum (stage II) with a dramatic increase for prolonged heat treatment and reaches saturation only after extensive annealing (stage III). At this point of heat treatment (point *B*), the electrical characteristics as a function of temperature exhibits semiconducting behavior.

The general behavior encountered in the electrical data is confirmed by optical absorption as measured by photothermal deflection spectroscopy (PDS), i.e., without employing electrodes and externally applied electrical fields. Figure 4 shows the absorption spectra of single crystalline $SrTiO_3$ after different annealing times and rapid cooling to room temperature in comparison with a spectrum of a crystal without heat treatment. The overall spectra are in good agreement with the literature (see, e.g., [23,29]). However, we found that the subgap absorption rises as a consequence of exposure to reducing conditions, but decreases again for extensive annealing. The optical spectra for other temperatures (between 700 and 1000 °C) differ concerning the absolute values of the subgap absorption, but the overall trend with the dramatic decrease for prolonged annealing

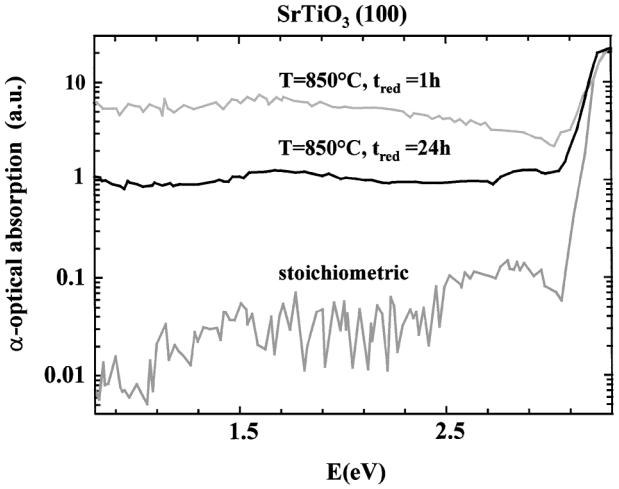

FIG. 4. Optical absorption spectra for as-received single crystals without and with reduction under vacuum conditions ($p_{O_2} = 1 \times 10^{-8}$ Torr) for different annealing times.

is very similar. In fact, in all cases the effect can already be recognized by visual inspection. Whereas the absorption spectra shown in Fig. 4 give evidence for a decreasing number of defects after prolonged annealing, the concomitant decrease of carrier concentration has been confirmed by infrared reflection measurements (not shown). As PDS is based on the heat generated by the absorption process, the time delay between the excitation and the signal increases with increasing distance of the heat source from the probe beam. From the analysis of the time delay for samples of different thickness it is concluded that the largest contributions of the subgap absorption stem only from the first few μm, consistent with the above-mentioned decrease in electrical conductivity within the skin region, and not from deeper parts of the crystals.

Combining the effusion experiments with the electrical and optical data gives evidence that prolonged annealing beyond the initial reduction (stage I) does not provide continued reduction of the crystals. Instead, an almost complete blocking of further exchange of oxygen with the surrounding atmosphere is encountered in stage II. We interpret this to be related to the redistribution of Sr and/or SrO complexes in the close neighborhood of the surface (within 10–50 nm) and subsequent solid state reactions [12,13] leading to a chemically inhomogeneous near-surface region which is characterized by nonperovskite phases such as TiO and Ti_2O, as well as Magnéli-type (Ti_mO_{2m-1}) and Ruddlesden-Popper phases [$SrO^*(SrTiO_3)_n$]. Further reduction gives rise to a decrease of the high local concentration of defect states and corresponding detectable free charge carriers in stage III. The observed breakdown of the metallic conductivity and decrease in optical subgap absorption cannot be related to only a local disruption of interconnections and formation of barriers within the metallic network. Besides a redistribution of vacancy defects by, e.g., multiplication of dislocations [30], one has probably to take into account structural changes such as collapse of the highly oxygen-deficient extended defects by a shearing mechanism [12,31].

In summary, our results give evidence that thermal reduction in single-crystalline $SrTiO_3$ is highly inhomogeneous in character and is governed by a complex interplay of counteracting processes. The observed metallic behavior for the moderate reducing conditions applied is shown to result from the preferential formation of vacancy defects along extended defects and their high density within the skin region. These phenomena necessitate a revision of the interpretation of the insulator-to-metal transition in reduced $SrTiO_3$ as well as probably the superconducting properties of this material. In particular, the density of induced charge carriers extracted on the basis of electrical or optical data have to be related to local properties. Our results also indicate that it may be impossible to homogeneously reduce single crystals of $SrTiO_3$ and describe their behavior in terms of standard point defect chemistry.

We appreciate the contribution by K. Schroeder to our understanding of the diffusivity along hierarchical trees of extended defects and gratefully acknowledge R. Waser for stimulating discussions.

[1] M. Imada, A. Fujimori, and Y. Tokura, Rev. Mod. Phys. **70**, 1039 (1998).
[2] C. Park and R. L. Snyder, J. Am. Ceram. Soc. **78**, 3171 (1995).
[3] P. A. Cox, *Transition Metal Oxides* (Clarendon Press, Oxford, 1995).
[4] P. Calvani *et al.,* Phys. Rev. B **47**, 8917 (1993).
[5] J. F. Schooley, W. R. Hosler, and M. L. Cohen, Phys. Rev. Lett. **12**, 474 (1964).
[6] J. K. Hulm *et al.,* in *Progress in Low Temperature Physics,* edited by C. J. Gorter (North-Holland Publishing Company, Amsterdam, London, 1970), Vol. VI, p. 205.
[7] T. Jarlborg, Phys. Rev. B **61**, 9887 (2000).
[8] P. Gumbsch *et al.,* Phys. Rev. Lett. **87**, 085505 (2001).
[9] R. Wang, Y. Zhu, and S. M. Shapiro, Phys. Rev. Lett. **80**, 2370 (1998).
[10] J. Philibert, *Atom Movements—Diffusion and Mass Transport in Solids* (Editions de Physique, Les Ulis, France, 1991).
[11] A. E. Paladino, L. G. Rubin, and J. S. Waugh, J. Phys. Chem. Solids **26**, 391 (1965).
[12] K. Szot and W. Speier, Phys. Rev. B **60**, 5909 (1999).
[13] K. Szot *et al.,* Appl. Phys. A **64**, 55 (1997).
[14] B. Stäuble-Pümpin *et al.,* Surf. Sci. **369**, 313 (1996).
[15] J. Yoshimura *et al.,* J. Cryst. Growth **191**, 483 (1998).
[16] K. Szot *et al.,* J. Phys. Chem. Solids **57**, 1765 (1996).
[17] I. Sakaguchi and H. Haneda, J. Solid State Chem. **124**, 195 (1996).
[18] We have convinced ourselves that the applied model assuming a constant density of subgrain boundaries also holds true in case of an inhomogeneous density distribution as a function of depth as long as saturation effects for oxygen at the dislocations line can be neglected.
[19] W. Beyer *et al.,* Philos. Mag. B **63**, 269 (1991).
[20] U. Balachandran and N. G. Eror, J. Solid State Chem. **39**, 351 (1981).
[21] N.-H. Chan, R. K. Sharma, and D. M. Smyth, J. Electrochem. Soc. **128**, 1762 (1981).
[22] P. Pasierb, S. Komornicki, and M. Rekas, J. Phys. Chem. Solids **60**, 1835 (1999).
[23] H. Yamada and G. R. Miller, J. Solid State Chem. **6**, 169 (1973).
[24] D. A. Crandles *et al.,* Phys. Rev. B **59**, 12 842 (1999).
[25] D. D. Sarma *et al.,* Europhys. Lett. **36**, 307 (1996).
[26] N. Shanthi and D. D. Sarma, Phys. Rev. B **57**, 2153 (1998).
[27] M. Kim *et al.,* Phys. Rev. Lett. **86**, 4056 (2001).
[28] The possible relation between extended defects and an induced transition from the insulating to metallic state has also been discussed in the case of electroreduced $KNbO_3$; see K. Szot, W. Speier, and W. Eberhardt, Appl. Phys. Lett. **60**, 1190 (1992).
[29] D. C. Lee, J. Destry, and J. L. Brebner, Phys. Rev. B **11**, 2299 (1975).
[30] J. P. Hirth and J. Lothe, *Theory of Dislocations* (Krieger Publishing Company, Malabar, FL, 1992).
[31] J. F. Banfield and D. R. Veblen, Am. Mineral. **77**, 545 (1992).